

# Geometrical and physical models of abrasion

G. Domokos

*Department of Mechanics, Materials, and Structures  
Budapest University of Technology and Economics*

*Müegyetem rkp.3  
Budapest 1111, Hungary  
and*

G. W. Gibbons

*D. A. M. T. P.*

*Cambridge University  
Wilberforce Road, Cambridge CB3 0WA, U.K.*

July 23, 2013

## Abstract

We extend the geometrical theory presented in [5] for collisional and frictional particle abrasion to include an independent physical equation for the evolution of mass and volume. We introduce volume weight functions as multipliers of the geometric equations and use these multipliers to enforce physical volume evolution in the unified equations. The latter predict, in accordance with Sternberg's Law, exponential decay for volume evolution. We describe both the PDE versions, which are generalisations of Bloore's equations and their heuristic ODE approximations, called the box equations. The latter are suitable for tracking the collective abrasion of large particle populations. The mutual abrasion of identical particles, called the self-dual flows, play a key role in explaining geological scenarios. We give stability criteria for the self-dual flows in terms of the parameters of the physical volume evolution models and show that under reasonable assumptions these criteria can be met by physical systems. We also study a natural generalisation, the Unidirectional Bloore equation, covering the case of unidirectional abrasion. We have previously shown that his equation admits travelling front solutions with circular profiles. More generally, in three dimensions, they are so-called linear or special Weingarten surfaces.

# Contents

<b>1</b>	<b>Introduction</b>	<b>3</b>
<b>2</b>	<b>Collisional abrasion of an individual particle in constant environment</b>	<b>4</b>
2.1	Bloore's Local Equation . . . . .	4
2.2	Level set representation . . . . .	5
2.3	Monge representation . . . . .	5
2.4	Relation to the Kardar-Parisi-Zhang equation . . . . .	6
2.5	Box Equations . . . . .	6
<b>3</b>	<b>Collisional abrasion of two, mutually colliding particles</b>	<b>7</b>
3.1	Binary Bloore Equations . . . . .	7
3.2	Binary Box Equations . . . . .	7
3.3	The self-dual flows . . . . .	7
3.4	The spherical case . . . . .	8
<b>4</b>	<b>Frictional abrasion of an individual particle: Non-local theory</b>	<b>8</b>
4.1	Bloore equations with friction . . . . .	8
4.2	Box equations with friction . . . . .	9
<b>5</b>	<b>Volume evolution in the geometric equations</b>	<b>9</b>
5.1	Geometric volume evolution in the Bloore equations: spherical case . . . . .	9
5.2	Geometric volume evolution in the box equations . . . . .	9
<b>6</b>	<b>Volume weighted individual and mutual abrasion</b>	<b>10</b>
6.1	Volume weighted Bloore Equations . . . . .	10
6.2	Volume weighted Box Equations . . . . .	10
6.3	Asymmetry of the volume weight function stabilising the self-dual flows . . . . .	11
6.4	Derivation of the volume weight function from physical models in the Bloore equations . . . . .	12
6.5	Derivation of the volume weight function from physical models in the box equations . . . . .	12
<b>7</b>	<b>Collective abrasion</b>	<b>13</b>
<b>8</b>	<b>Physical models of mass evolution</b>	<b>13</b>
8.1	Collisional Models . . . . .	13
8.2	Frictional models . . . . .	15
8.3	Collective abrasion: rescaling of time . . . . .	15
<b>9</b>	<b>Lifetimes, Sternberg's Law and the stability of the self-dual flows</b>	<b>16</b>
9.1	Lifetimes, physical mass evolution models and Sternberg's Law . . . . .	16
9.2	Lifetimes and the volume weight functions . . . . .	16
9.3	Stability of the self-dual flows in the stochastic process . . . . .	17
<b>10</b>	<b>Acknowledgements</b>	<b>18</b>
<b>11</b>	<b>Appendix: Uni-directional Bloore Flows and Weingarten Surfaces</b>	<b>19</b>
11.1	Weingarten surfaces as translators . . . . .	20
<b>12</b>	<b>Appendix: Observable quantities in the geometric equations</b>	<b>20</b>
12.1	Self-similar evolution . . . . .	21
12.2	Observable quantities in the geometrical box flows . . . . .	22
12.2.1	Eikonal flow . . . . .	22
12.2.2	Mean Curvature Flow . . . . .	22
12.2.3	Gaussian Flow . . . . .	23

# 1 Introduction

In our earlier paper [5] we investigated Bloore’s collisional partial differential equation (PDE) [1] describing the evolution of particle shapes under isotropic collisions:

$$-v = a(1 + 2bH + cK) \quad (1)$$

where  $v$  is the evolution speed in the direction of the inward normal,  $a = \text{constant}$  with the dimension of speed,  $H = \frac{1}{2}(k_1 + k_2)$  is the mean curvature and  $K = \kappa_1\kappa_2$  is the Gauss curvature and  $b$  and  $c$  are constants with the dimensions of length and length<sup>2</sup> respectively. In [5] we approximated (1) by a set of ordinary differential equations called the box equations under the assumption that all shapes are ellipsoidal and remain so for all times, i.e. it is sufficient to track the evolution of the orthogonal bounding boxes. The box model was successfully tested against laboratory experiments and recently against a detailed field study along the Williams river, Australia [34].

In the current paper we extend and generalise our previous work. The original Bloore equation (1) and its box approximations correctly describe the evolution of geometrical shapes, however, these are purely geometrical equations and thus unable to predict the correct time evolution for mass and volume. One important sign of this shortcoming is that the model (1) predicts finite lifetimes for all particles whereas field observations in fluvial environments indicate an exponential decay as formulated by Sternberg’s empirical formula, also called Sternberg’s Law [4]. This indicates that volume evolution has to be derived from physical equations independent of the Bloore model.

Although physically incorrect, the Bloore model (and its box approximations) still predict volume evolution rates depending on the normal speed  $v$  from (1) and on the geometry of the surface  $\Sigma$ :

$$\dot{V}^g(v) = \int_{\Sigma} v dA. \quad (2)$$

where the superscript  $g$  refers to the geometrical equations and  $\dot{(\ )}$  denotes differentiation with respect to time. These rates we call *the geometrical volume evolution* and we derive the exact formulae in section 5. As we can see in (2),  $\dot{V}^g$  is a linear function of the normal speed  $v$  in (1), i.e.

$$\dot{V}^g(\lambda v) = \lambda \dot{V}^g. \quad (3)$$

Subsequently, in section 6 in the spirit of Firey’s work [14] we introduce the *volume weight functions*  $f(V(t))$  which depend only on time and do not depend on the location on the surface. These functions enter Bloore’s equation instead of the constant  $a$  and we also define their analogues in the box equations. If we have an independent physical model for volume evolution predicting volume diminution rate  $\dot{V}^p$  (the superscript referring to the independent physical equations) then we can set this equal to the volume diminution predicted by the volume-weighted geometrical equations

$$\dot{V}^g(f(V)v) = \dot{V}^p \quad (4)$$

and this condition yields, via the linear property (3)

$$f(V) = \frac{\dot{V}^p}{\dot{V}^g}. \quad (5)$$

This illustrates that volume weight functions can be used to suppress the geometrical volume evolution rates entirely in favour of the physical ones. After introducing in section 7 the basic equations for the statistical theory of collective abrasion, in section 8 we introduce some models which predict physical volume diminution in accordance with Sternberg’s Law, so combining these models with the original geometrical equations via the volume weight functions yields shape and size evolution consistent both with the geometrical Bloore theory as well as Sternberg’s empirical formula for volume diminution.

In addition to introducing the volume weight functions and the physical volume evolution into the geometrical model, we also generalise the original Bloore model in other ways. In section 3 we introduce the coupled system of PDEs describing the mutual abrasion of two particles, as well as the box approximations of these equations. All previously mentioned equations deal with collisional abrasion which, as we pointed out in [5] is not capable on its own to adequately describe the collective evolution of pebbles in geological environments. In section 4 we introduce the PDE including friction and also its box approximations. In section 8 we also provide the physical volume evolution model for the frictional case.

Frictional abrasion is particularly significant, because in [5] we showed that in the box flows if identical shapes mutually abrade each other (which we call the self-dual flow) then friction may stabilise nontrivial shapes as global attractors. However, it was not clear whether these shapes are also attractive in size, i.e. whether the self-dual flows are stable with

respect to perturbations in size. Earlier we pointed out that global transport resulting in size segregation may stabilise these flows. While that is certainly a valid possibility, in section 9 we show that a potentially more relevant mechanism is defined by the physical models of volume diminution. In the models introduced in our current paper we show the exact condition under which a physical volume diminution model can stabilise the self-dual flows.

Beyond isotropic particle abrasion we also discuss unidirectional abrasion and in Appendix 11 we show that under such conditions linear Weingarten surfaces emerge as translationally invariant solutions of the unidirectional Bloore equation.

The current version of the manuscript is intended to convey both the theoretical PDE models based on Bloore's equation as well as to provide detailed basis for a computer code simulating collective abrasion based on the box equations. The latter could serve as a platform to compare these results with field data and laboratory data. Due to this double goal, readers interested in any one of the above subjects may find some equations which appear less relevant to their immediate purpose. On the other hand, separation of the two subjects also raises difficulties and at this stage we decided to keep the material at least temporarily unified.

## 2 Collisional abrasion of an individual particle in constant environment

### 2.1 Bloore's Local Equation

In [1] Bloore proposed that the shape of the bounding surface  $\Sigma$  of pebbles made of a homogeneous material and eroded by a gas of small spherical abraders should be governed by a local equation of the form

$$-v = F(\kappa_1, \kappa_2), \quad (6)$$

where  $\kappa_1, \kappa_2 = \frac{1}{R_1}, \frac{1}{R_2}$  and  $R_1, R_2$  are the principal radii of curvatures,  $v$  is the speed along the inward normal at which the local area element  $dA$  is being eroded and  $F(\kappa_1, \kappa_2)$  is some symmetric function of the principal curvatures  $\kappa_1, \kappa_2$ . The simplest case is perhaps (1), mentioned in the Introduction. For spherical abraders of radius  $r$ , Bloore gave a statistical argument that

$$b = r, \quad c = r^2. \quad (7)$$

For non-spherical abraders, a more sophisticated treatment using Schneider-Weil theory [8] leads to

$$b = \frac{M}{4\pi}, \quad c = \frac{A}{4\pi}, \quad (8)$$

where

$$M = \int_{\Sigma} H dA, \quad A = \int_{\Sigma} dA \quad (9)$$

are the integrated mean curvature and area respectively. Thus one expects on purely dimensional grounds that the first term to be important for pebbles whose linear size is large compared with the size of the abraders while for pebbles whose linear size is comparable with the size of the abraders the second and third terms should be increasingly important. Evidently, when the size of the pebble is comparable with the size of the abraders, the *single pebble* treatment like Bloore's breaks down and the evolution of the abraders must also be considered.

In the mathematics literature the three terms in (1) are often treated separately. The first term in (1)

$$-v = a \quad (10)$$

is called the *Eikonal equation* or the *parallel map* and arises in the study of wave fronts with speed  $a$ , satisfying Huygens's principle. Given an initial aspherical surface the Eikonal flow tends to make the surface more aspherical and to develop faces which intersect on edges [2].

The second term in (1)

$$-v = 2abH \quad (11)$$

is called the *mean curvature flow* [3] and often arises in problems where surface tension is important [3, 24]. Given an initial aspherical surface it tends to make the surface more spherical [23].

The third term in (1)

$$-v = acK \quad (12)$$

is called the *Gauss flow* and it also tends to make the surface more spherical [19, 20, 21].

For completeness we mention a fourth flow which is sometimes studied for its special mathematical properties [22] which we call the *Rayleigh* flow

$$-v = \text{constant} K^{\frac{1}{4}}. \quad (13)$$

The reason for our name is that this flow has the property, first noticed by Lord Rayleigh [15, 16, 17] that under it, ellipsoids evolve in a self-similar fashion.

## 2.2 Level set representation

If we describe the moving shape  $\Sigma$  as the level sets

$$t + \phi(x, y, z) = 0, \quad (14)$$

we may transcribe a Bloore type equation for the moving surface  $\Sigma$  as a PDE for  $\phi(x, y, z)$  as follows. In one time step

$$dt + \nabla \phi \cdot d\mathbf{r} = 0. \quad (15)$$

where  $\mathbf{r} = [x, y, z]^T$  is the position vector defining the surface. Thus we have

$$1 + \nabla \phi \cdot \frac{d\mathbf{r}}{dt} = 0. \quad (16)$$

But the velocity  $v$  in the normal direction is

$$v = \frac{d\mathbf{r}}{dt} \cdot \frac{\nabla \phi}{|\nabla \phi|} \quad (17)$$

Thus

$$1 + |\nabla \phi|v = 0. \quad (18)$$

where  $v = v(\kappa_1, \kappa_2)$  and  $\kappa_1, \kappa_2$  may be expressed in terms of  $\phi$  (see e.g. [33]). In particular

$$\begin{aligned} H &= \frac{1}{2} \nabla \cdot \frac{\nabla \phi}{|\nabla \phi|} \\ K &= \frac{G}{(\phi_x^2 + \phi_y^2 + \phi_z^2)^2} \\ G &= \phi_x^2(\phi_{yy}\phi_{zz} - \phi_{yz}^2) + \phi_y^2(\phi_{zz}\phi_{xx} - \phi_{zx}^2) + \phi_z^2(\phi_{xx}\phi_{yy} - \phi_{xy}^2) \\ &\quad + 2\phi_x\phi_y(\phi_{xz}\phi_{yz} - \phi_{xy}\phi_{zz}) + 2\phi_y\phi_z(\phi_{yx}\phi_{zx} - \phi_{yz}\phi_{xx}) + 2\phi_z\phi_x(\phi_{zy}\phi_{xy} - \phi_{zx}\phi_{yy}) \end{aligned} \quad (19)$$

and of course we have

$$\kappa_{1,2} = H \pm \sqrt{H^2 - K}. \quad (20)$$

## 2.3 Monge representation

Following Monge [32], if  $\Sigma$  is a single-valued function in  $(x, y)$  then we may represent it as a graph over a plane

$$z - h(x, y, t) = 0. \quad (21)$$

Since the normal is  $\frac{1}{\sqrt{1+h_x^2+h_y^2}}(-h_x, -h_y, 1)$  we obtain the Bloore equation as a PDE in  $x, y, t$

$$\frac{\partial h}{\partial t} = \frac{1}{\sqrt{1+h_x^2+h_y^2}}v. \quad (22)$$

The standard expressions for  $H$  and  $K$  may be obtained by substituting  $\phi = z - h(x, y, t)$  in (19).

$$\begin{aligned} K &= \frac{h_{xx}h_{yy} - h_{xy}^2}{(1+h_x^2+h_y^2)^2} \\ H &= \frac{1}{2} \frac{(1+h_y^2)h_{xx} + (1+h_x^2)h_{yy} - 2h_xh_yh_{xy}}{(1+h_x^2+h_y^2)^{\frac{3}{2}}}, \end{aligned} \quad (23)$$

An interesting application of both sets of formulae is to the surface

$$xyz = c, \quad \iff \quad z = \frac{c}{xy} \quad (24)$$

for which

$$K = \frac{3c^3}{(x^2y^2 + y^2z^2 + z^2x^2)^2} \quad (25)$$

$$H = -\frac{c(x^2 + y^2 + z^2)}{(y^2z^2 + z^2x^2 + x^2y^2)^{3/2}} \quad (26)$$

Interestingly, this family of surfaces is invariant under the Rayleigh flow (13) since it is a Titzeica surface, that is the stutz or support function  $\mathbf{x} \cdot \mathbf{n}$  is constant multiple of  $K^{1/4}$ .

## 2.4 Relation to the Kardar-Parisi-Zhang equation

In soft condensed matter physics, interfaces are often modelled using the the *Kardar-Parisi-Zhang equation* for the height function  $h = h(x, y)$

$$\frac{\partial h}{\partial t} = \nu \nabla^2 h + \frac{\lambda}{2} (\nabla h)^2 + \eta(x, y, t) \quad (27)$$

where  $\nabla$  is with respect to the *flat* metric on  $\mathbb{E}^2$  and  $\eta(x, y, t)$  is a Langevin-type stochastic Gaussian noise term [28, 29]. It was pointed out in [30] that this was not re-parametrisation invariant and is an approximation to a stochastic version of the *mean curvature flow*.

$$v = -\nu H + \lambda + \eta(\sigma^A, t) \quad (28)$$

The first term is essentially the functional derivative of surface energy, i.e. a *surface tension term* and the second is the functional derivative of a volume energy i.e. a *pressure* term. In the absence of the stochastic noise, i.e. if  $\eta = 0$  and if  $\nu, \lambda > 0$ , the system should relax to a surface of constant mean curvature  $H = \frac{\lambda}{\nu}$ . For pebbles  $\lambda = a$  and  $\nu = -2ab$  and the pressure is negative. In the absence of the noise term, the KPZ equation (27) may, by means of the substitution  $w = \exp(\frac{\lambda}{2\nu}h)$ , reduced to the linear diffusion equation for  $w$  [31].

## 2.5 Box Equations

The Bloore equations are partial differential equations and define a flow on the infinite space of shapes. In [5] a finite dimensional truncation was introduced which leads to a finite number of ordinary differential equations referred to as the *box equations*. The basic idea is to bound our pebble by rectangular box of sides  $2u_1, 2u_2, 2u_3$  ordered such that  $u_1 \leq u_2 \leq u_3$  which defines an inscribed ellipsoid of semi-axes  $u_1, u_2, u_3$ . One then writes down three equations

$$-\dot{u}_i = F(\kappa_{1i}, \kappa_{2i}) \quad (29)$$

where  $i = 1, 2, 3$  and  $\kappa_{1i}, \kappa_{2i}$  are now taken to be the curvatures of the inscribed ellipsoid at the ends of the three principal axes  $(\pm u_1, 0, 0), (0, \pm u_2, 0), (0, 0, \pm u_3)$ . Thus (1) takes the form

$$-\dot{u}_1 = a \left( 1 + b \left( \frac{u_1}{u_2^2} + \frac{u_1}{u_3^2} \right) + c \frac{u_1^2}{u_2^2 u_3^2} \right), \quad \text{etc} \quad (30)$$

where etc denotes two further equations obtained by cyclic permutation of the suffices 1, 2, 3.

In [5] it was found convenient to replace the three lengths  $u_1, u_2, u_3$  by two dimensionless ratios and a length  $y_1 = \frac{u_1}{u_3}$ ,  $y_2 = \frac{u_2}{u_3}$  and  $y_3 = u_3$ , yielding

$$\dot{y}_i = a F_i^E(y_1, y_2, y_3, b, c) = a \left( \frac{F_i^E}{y_3} + 2b \frac{F_i^M}{y_3^2} + c \frac{F_i^G}{y_3^3} \right) \quad (31)$$

$$-\dot{y}_3 = a F_3(y_1, y_2, y_3, b, c) = a \left( 1 + \frac{b}{y_3} \frac{y_1^2 + y_2^2}{y_1^2 y_2^2} + \frac{c}{y_3^2} \frac{1}{y_1^2 y_2^2} \right), \quad (32)$$

where

$$F_i^E = y_i - 1, \quad F_i^M = \frac{1 - y_i^2}{2y_i} \quad F_i^G = \frac{1 - y_i^3}{y_i y_j^2}, \quad i, j = 1, 2; i \neq j. \quad (33)$$

By introducing the vector notation  $\mathbf{y} = [y_1, y_2, y_3]^T$ ,  $\mathbf{F} = [F_1, F_2, F_3]^T$ , (31)-(32) can be rewritten as

$$\dot{\mathbf{y}} = a\mathbf{F}(\mathbf{y}, b, c), \quad (34)$$

which is identical to equations (2.2)-(2.6) of [5].

A special case of the box equations are the *spherical flows* for which  $u_1 = u_2 = u_3 = R$ , where  $R$  is the radius of the sphere. The spherical flows obtained from the box equations in fact coincide with the exact solutions of the full partial differential equations (1) obtained by assuming that  $\Sigma$  is a sphere.

### 3 Collisional abrasion of two, mutually colliding particles

#### 3.1 Binary Bloore Equations

In the Bloore equations the abraders are assumed to be constant in shape and size. It is, however, simple to write down a set of evolution equations for both the abraders and the abraded pebbles as done in [5] for the simplified case, the box equations. In that case we introduced semi-box-lengths  $v_1, v_2, v_3$  for the abrading particles, yielding two dimensionless ratios and one length  $z_1 = \frac{v_1}{v_3}$ ,  $z_2 = \frac{v_2}{v_3}$  and  $z_3 = v_3$ . Retaining the notation of [5] we use the labels  $y$  and  $z$  for abraded and abraded, by utilising (8), the obvious partial differential equations to consider are

$$-v_y = a \left( 1 + 2 \frac{M_z}{4\pi} H_y + \frac{A_z}{4\pi} K_y \right) \quad (35)$$

$$-v_z = a \left( 1 + 2 \frac{M_y}{4\pi} H_z + \frac{A_y}{4\pi} K_z \right). \quad (36)$$

#### 3.2 Binary Box Equations

In the box approximation the mean curvature and surface area integrals in (8) are replaced by the corresponding quantities of the orthogonal bounding box of the the incoming particle (which, for simplicity is now taken as the  $\mathbf{z}$  particle):

$$M = 2\pi z_3(z_1 + z_2 + 1), \quad A = 8z_3^2(z_1 z_2 + z_1 + z_2). \quad (37)$$

The same quantities can be expressed for the unit cube as  $M_1 = 6\pi$ ,  $A_1 = 24$ , so in the box equations we have

$$b(\mathbf{z}) = \frac{M}{M_1} = z_3 \frac{z_1 + z_2 + 1}{3} = z_3 f_z^b, \quad c(\mathbf{z}) = \frac{A}{A_1} = z_3^2 \frac{z_1 + z_2 + z_1 z_2}{3} = z_3^2 f_z^c. \quad (38)$$

The corresponding binary box equations can be written as

$$\dot{\mathbf{y}} = a\mathbf{F}(\mathbf{y}, b(\mathbf{z}), c(\mathbf{z})) = a\mathbf{F}^c(\mathbf{y}, \mathbf{z}) \quad (39)$$

$$\dot{\mathbf{z}} = a\mathbf{F}(\mathbf{z}, b(\mathbf{y}), c(\mathbf{y})) = a\mathbf{F}^c(\mathbf{z}, \mathbf{y}) \quad (40)$$

where superscript  $c$  refers to collisional abrasion. Equations (39)-(40) are similar to equations (2.13)-(2.14) of [5].

#### 3.3 The self-dual flows

As written, the equations (35)-(36) have a solution for which the abraders and abraded have identical forms. This solution we refer to as the *self-dual flow*. For the self-dual flow the labels  $y$  and  $z$  are redundant and we are left with the single equation

$$-v = a \left( 1 + 2 \frac{M}{4\pi} H + \frac{A}{4\pi} K \right) \quad (41)$$

which in the box approximation reads

$$\dot{\mathbf{y}} = a\mathbf{F}(\mathbf{y}, b(\mathbf{y}), c(\mathbf{y})) = a\mathbf{F}^c(\mathbf{y}, \mathbf{y}). \quad (42)$$

An important question is whether the self dual flow (41) or its box version (42) are stable within the class of Binary Bloore flows (35)-(36) and Binary Box flows (39)-(40), respectively.

### 3.4 The spherical case

If both particles are spherical (with radii  $R_y$  and  $R_z$ , respectively), then both the binary Bloore equations (35)-(36) and the binary box equations (39)-(40) collapse to the same two coupled first order ordinary differential equations:

$$-\dot{R}_y = a \left( 1 + 2\frac{R_z}{R_y} + \left(\frac{R_z}{R_y}\right)^2 \right) \quad (43)$$

$$-\dot{R}_z = a \left( 1 + 2\frac{R_y}{R_z} + \left(\frac{R_y}{R_z}\right)^2 \right). \quad (44)$$

## 4 Frictional abrasion of an individual particle: Non-local theory

### 4.1 Bloore equations with friction

In [5] the effects of mutual friction, both rolling and sliding were incorporated into the box equations. This can be done at the level of the equations describing the the complete evolution of the pebble but while the equations remain first order in time they become rather non-local in the coordinates  $u, v$  used to parametrise the embedding

$$\mathbf{r} = \mathbf{r}(u, v, t) \quad (45)$$

of the surface  $\Sigma$  into Euclidean space.

We define  $R(u, v, t) = |\mathbf{r}(u, v, t) - \bar{\mathbf{r}}(t)|$  to be the distance of the point  $\mathbf{r}(u, v, t)$  from the instantaneous centroid  $\bar{\mathbf{r}}(t)$  of the pebble. We also define  $R_{\max}(t)$  and  $R_{\min}(t)$  as the instantaneous maximum and minimum of values of  $R(u, v, t)$  over the surface and we postulate that frictional abrasion is governed by

$$\frac{\partial \mathbf{r}(u, v, t)}{\partial t} = -G(R, R_{\min}, R_{\max}) \mathbf{n}(u, v, t), \quad G > 0. \quad (46)$$

In [5] several constraints on the general form of of the function  $G(R, R_{\min}, R_{\max})$  were given and also one example satisfying these constraints was demonstrated, introducing separate terms for sliding and rolling with independent coefficients  $\nu_s, \nu_r$ , respectively and the dimensionless ratios  $r_1 = R/R_{\min}, r_2 = R/R_{\max}$ :

$$G(R, R_{\min}, R_{\max}) = \nu_s f_s(r_1, r_2) + \nu_r f_r(r_1, r_2) = \nu_s r_2 r_1^{-n} + \nu_r r_2 (1 - r_2^n). \quad (47)$$

According to the arguments discussed in [5], for sufficiently high values of  $n$ , this model appears to capture most essential physical features of frictional abrasion. While (47) is clearly just an example ([5] describes also an alternative equation), however, it provides a simple basis for a qualitative analysis.

Frictional abrasion can be readily introduced into the Bloore equations. As before we use the labels  $y$  and  $z$ . Since friction is an *additional independent* mechanism for abrasion it is natural to assume that

$$-v_y = a \left( 1 + 2\frac{M_z}{4\pi} H_y + \frac{A_z}{4\pi} K_y \right) + G(R_y, R_{y \min}, R_{y \max}), \quad (48)$$

$$-v_z = a \left( 1 + 2\frac{M_y}{4\pi} H_z + \frac{A_y}{4\pi} K_z \right) + G(R_z, R_{z \min}, R_{z \max}). \quad (49)$$

In case of spherical flows (47) reduces to a single constant  $\nu_s$ , so we have

$$-\dot{R}_y = a \left( 1 + 2\frac{R_z}{R_y} + \left(\frac{R_z}{R_y}\right)^2 \right) + \nu_s, \quad (50)$$

$$-\dot{R}_z = a \left( 1 + 2\frac{R_y}{R_z} + \left(\frac{R_y}{R_z}\right)^2 \right) + \nu_s. \quad (51)$$

## 4.2 Box equations with friction

If we take the  $n \rightarrow \infty$  limit in the semi-local PDE (47) we obtain for the box variables

$$\dot{u}_1 = -\nu_s y_1 - \nu_r y_1, \quad \dot{u}_2 = -\nu_r y_2, \quad \dot{u}_3 = 0, \quad (52)$$

where  $\nu_s, \nu_r$  are the coefficients for sliding and rolling friction, respectively. Equation (52) is equivalent to

$$\dot{\mathbf{y}} = \mathbf{F}^f(\mathbf{y}, \nu_s, \nu_r) = \frac{1}{y_3}(\nu_s \mathbf{F}^S + \nu_r \mathbf{F}^R), \quad (53)$$

where

$$\mathbf{F}^S = -[y_1, 0, 0]^T, \quad \mathbf{F}^R = -[y_1, y_2, 0]^T. \quad (54)$$

We can now simply add collisional and frictional flows (39)-(40) and (53) to obtain the collisional-frictional equations for the two-body problem:

$$\dot{\mathbf{y}} = a\mathbf{F}^c(\mathbf{y}, \mathbf{z}) + \mathbf{F}^f(\mathbf{y}, \nu_s, \nu_r) \quad (55)$$

$$\dot{\mathbf{z}} = a\mathbf{F}^c(\mathbf{z}, \mathbf{y}) + \mathbf{F}^f(\mathbf{z}, \nu_s, \nu_r). \quad (56)$$

## 5 Volume evolution in the geometric equations

### 5.1 Geometric volume evolution in the Bloore equations: spherical case

The Binary Bloore equations (35)-(36) define the mutual evolution of *observable quantities*, such as maximal width  $D$ , surface area  $A$  and volume  $V$ . In general, we can not obtain closed formulae for their evolution, however, the spherical case admits such computations. In case of spherical particles with radii  $R_y, R_z$  volume evolution can be derived by integrating (43)-(44) on the surface, to obtain

$$-\dot{V}_y = -\dot{V}_z = 4a\pi(R_y + R_z)^2 \quad (57)$$

which we call the *geometrical volume evolution* for spheres in the binary Bloore equations.

### 5.2 Geometric volume evolution in the box equations

In the box equations we can derive geometric volume evolution for arbitrary shapes. Regardless whether the abrasion is collisional or frictional, the volumes  $V_y, V_z$  of the two particles can be expressed as

$$V_y = 8y_1 y_2 y_3^3, \quad (58)$$

$$V_z = 8z_1 z_2 z_3^3. \quad (59)$$

By differentiating (58)-(59) with respect to time we get for the geometric volume evolution:

$$\dot{V}_y^g(\mathbf{y}, \dot{\mathbf{y}}) = \frac{d}{dt}(8y_1 y_2 y_3^3) = 8(\dot{y}_1 y_2 y_3^3 + y_1 \dot{y}_2 y_3^3 + 3y_1 y_2 y_3^2 \dot{y}_3), \quad (60)$$

$$\dot{V}_z^g(\mathbf{z}, \dot{\mathbf{z}}) = \frac{d}{dt}(8z_1 z_2 z_3^3) = 8(\dot{z}_1 z_2 z_3^3 + z_1 \dot{z}_2 z_3^3 + 3z_1 z_2 z_3^2 \dot{z}_3), \quad (61)$$

and we note that  $\dot{V}_y^g, \dot{V}_z^g$  are linear in  $\dot{\mathbf{y}}, \dot{\mathbf{z}}$ , respectively, i.e.

$$\lambda \dot{V}_y^g(\mathbf{y}, \dot{\mathbf{y}}) = \dot{V}_y^g(\mathbf{y}, \lambda \dot{\mathbf{y}}), \quad (62)$$

and the same holds for  $\dot{V}_z^g$ . Now we substitute the collisional equations (39)-(40) into (60)-(61) to obtain the geometric volume evolution specifically for collisional abrasion

$$\dot{V}_y^{g,c}(\mathbf{y}, \dot{\mathbf{y}}) = \dot{V}_y^{g,c}(\mathbf{y}, a\mathbf{F}^c(\mathbf{y}, \mathbf{z})) = aF^{g,c}(\mathbf{y}, \mathbf{z}) \quad (63)$$

$$\dot{V}_z^{g,c}(\mathbf{z}, \dot{\mathbf{z}}) = \dot{V}_z^{g,c}(\mathbf{z}, a\mathbf{F}^c(\mathbf{z}, \mathbf{y})) = aF^{g,c}(\mathbf{z}, \mathbf{y}). \quad (64)$$

The geometric volume evolution under friction can be derived similarly to its collisional counterpart in (63)-(64):

$$\dot{V}_y^{g,f}(\mathbf{y}, \dot{\mathbf{y}}) = \dot{V}_y^{g,f}(\mathbf{y}, \mathbf{F}^f(\mathbf{y}, \nu_s, \nu_r)) = F^{g,f}(\mathbf{y}, \nu_s, \nu_r) \quad (65)$$

$$\dot{V}_z^{g,f}(\mathbf{z}, \dot{\mathbf{z}}) = \dot{V}_z^{g,f}(\mathbf{z}, \mathbf{F}^f(\mathbf{z}, \nu_s, \nu_r)) = F^{g,f}(\mathbf{z}, \nu_s, \nu_r). \quad (66)$$

where  $\mathbf{F}^f$  is from (53). We can also compute  $F^{g,f}(\mathbf{y}, \nu_s, \nu_r)$  explicitly by substituting (53)-(54) into (60):

$$F^{g,f}(\mathbf{y}, \nu_s, \nu_r) = \dot{V}^{g,f} = \frac{f_1^f}{y_3} y_2 y_3^3 + \frac{f_2^f}{y_3} y_1 y_3^3 + 3f_3^f y_1 y_2 y_3^2 = -\frac{V_y}{y_3} (\nu_s + 2\nu_r) \quad (67)$$

where

$$f_1^f(y_1, y_2, \nu_1, \nu_2) = \nu_s F_1^S + \nu_r F_1^R = -\nu_s y_1 - \nu_r y_1 \quad (68)$$

$$f_2^f(y_1, y_2, \nu_1, \nu_2) = \nu_s F_2^S + \nu_r F_2^R = -\nu_r y_2 \quad (69)$$

$$f_3^f(y_1, y_2, \nu_1, \nu_2) = \nu_s F_3^S + \nu_r F_3^R = 0. \quad (70)$$

## 6 Volume weighted individual and mutual abrasion

### 6.1 Volume weighted Bloore Equations

Bloore's general equation (6) and its particular case (1) are local in character and did not take into account the possibility that non-local properties of the pebble might influence the speed of abrasion  $v$ . In fact, three years before Bloore, Firey [14] had studied a modification of the Gauss flow (12) of the form

$$-v = \alpha V^p K, \quad (71)$$

where  $V$  is the volume of the pebble and  $\alpha$  and  $p$  are constants. Based on some experimental work [18] consistent with the intuition that more massive pebbles should abrade faster than less massive particles, Firey chose  $p = 1$ . More generally one might consider replacing (1) by

$$-v = f(V)(1 + 2bH + cK) \quad (72)$$

where  $f(V)$  may be considered as a variable speed of attrition for the Eikonal term depending on the mass of equivalently the volume  $V$  of the pebble. We can introduce the volume weight functions in the Binary Bloore flows (35)-(36) as:

$$-v_y = f^c(V_y, V_z) \left( 1 + 2\frac{M_z}{4\pi} H_y + \frac{A_z}{4\pi} K_y \right) \quad (73)$$

$$-v_z = f^c(V_z, V_y) \left( 1 + 2\frac{M_y}{4\pi} H_z + \frac{A_y}{4\pi} K_z \right) \quad (74)$$

and in case of spherical particles, based on (43)-(44), this reduces to

$$-\dot{R}_y = f^c(V_y, V_z) \left( 1 + 2\frac{R_z}{R_y} + \left( \frac{R_z}{R_y} \right)^2 \right) \quad (75)$$

$$-\dot{R}_z = f^c(V_z, V_y) \left( 1 + 2\frac{R_y}{R_z} + \left( \frac{R_y}{R_z} \right)^2 \right). \quad (76)$$

In case of both collisional and frictional abrasion we have

$$-v_y = f^c(V_y, V_z) \left( 1 + 2\frac{M_z}{4\pi} H_y + \frac{A_z}{4\pi} K_y \right) + f^f(V_y) G(R_y, R_{y \min}, R_{y \max}) \quad (77)$$

$$-v_z = f^c(V_z, V_y) \left( 1 + 2\frac{M_y}{4\pi} H_z + \frac{A_y}{4\pi} K_z \right) + f^f(V_z) G(R_z, R_{z \min}, R_{z \max}), \quad (78)$$

### 6.2 Volume weighted Box Equations

In the box equation approximation one has  $V = V(\mathbf{y}) = 8y_1 y_2 y_3^3$  and (34) becomes

$$\dot{\mathbf{y}} = f(V(\mathbf{y})) \mathbf{F}(\mathbf{y}, b, c). \quad (79)$$

Evidently, the path pursued by a pebble in the space of shapes is unaffected by the prefactor  $f(V)$  in (72) merely the speed with which the curve is executed.

We can introduce the volume weight functions in the Binary Box flows (39)-(40) as:

$$\dot{\mathbf{y}} = f^c(V_y(\mathbf{y}), V_z(\mathbf{z}))\mathbf{F}^c(\mathbf{y}, \mathbf{z}) = f^c(\mathbf{y}, \mathbf{z})\mathbf{F}^c(\mathbf{y}, \mathbf{z}) = \hat{\mathbf{F}}^c(\mathbf{y}, \mathbf{z}) \quad (80)$$

$$\dot{\mathbf{z}} = f^c(V_z(\mathbf{z}), V_y(\mathbf{y}))\mathbf{F}^c(\mathbf{z}, \mathbf{y}) = f^c(\mathbf{z}, \mathbf{y})\mathbf{F}^c(\mathbf{z}, \mathbf{y}) = \hat{\mathbf{F}}^c(\mathbf{z}, \mathbf{y}) \quad (81)$$

where  $\hat{\cdot}$  indicates that the volume weight is included in the operator. The linear behaviour (62) and equations (63)-(64) imply that in the volume weighted box equations (80)-(81) volume evolution will be given by

$$\dot{V}_y^{g,c}(\mathbf{y}, \dot{\mathbf{y}}) = \dot{V}_y^{g,c}(\mathbf{y}, f^c(\mathbf{y}, \mathbf{z})\mathbf{F}^c(\mathbf{y}, \mathbf{z})) = f^c(\mathbf{y}, \mathbf{z})F^{g,c}(\mathbf{y}, \mathbf{z}) \quad (82)$$

$$\dot{V}_z^{g,c}(\mathbf{z}, \dot{\mathbf{z}}) = \dot{V}_z^{g,c}(\mathbf{z}, f^c(\mathbf{z}, \mathbf{y})\mathbf{F}^c(\mathbf{z}, \mathbf{y})) = f^c(\mathbf{z}, \mathbf{y})F^{g,c}(\mathbf{z}, \mathbf{y}) \quad (83)$$

where  $\hat{\cdot}$  refers to the inclusion of the volume weight function and  $F^{g,c}$  is given in (63). We introduce the volume weight function in an analogous manner for frictional abrasion based on (53):

$$\dot{\mathbf{y}} = f^f(V_y(\mathbf{y}))\mathbf{F}^f(\mathbf{y}, \nu_s, \nu_r) = f^f(\mathbf{y})\mathbf{F}^f(\mathbf{y}, \nu_s, \nu_r) = \hat{\mathbf{F}}^f(\mathbf{y}, \nu_s, \nu_r) \quad (84)$$

and again  $\hat{\cdot}$  indicates that the volume weight is included in the operator. Here again (62) and (65)-(66) imply that in volume weighted frictional box equation (84) volume evolution is given by:

$$\dot{V}_y^{g,f}(\mathbf{y}, \dot{\mathbf{y}}) = \dot{V}_y^{g,f}(\mathbf{y}, f^f(\mathbf{y})\mathbf{F}^f(\mathbf{y}, \nu_s, \nu_r)) = f^f(\mathbf{y})F^{g,f}(\mathbf{y}, \nu_s, \nu_r) \quad (85)$$

where  $F^{g,f}$  is given in (67) and  $\dot{V}_z^{g,f}(\mathbf{z}, \dot{\mathbf{z}})$  is defined in the same manner.

Our next goal is to derive the volume weight function  $f(V_y, V_z)$  for the Binary Bloore Flows (73)-(74) and Binary Box Flows (80)-(81), based on some physical considerations and to investigate the stability of the volume-weighted self-dual flows. The PDE (73)-(74) only admits the study of the special case where both particles are spherical and we will derive the volume weight function for this case. Subsequently, in an analogous manner, we will identify the volume weight function for general (non-spherical) particle evolution in the box equations (80)-(81).

### 6.3 Asymmetry of the volume weight function stabilising the self-dual flows

Before introducing the physical considerations, we point out, purely on geometric grounds, a fundamental property of the volume weight function  $f$ : in order to stabilise the self-dual collisional flows,  $f$  needs to be asymmetrical. It is sufficient to show in the spherical case that the symmetric volume weight function implies instability.

The spherical flow (75)-(76) takes place in the positive quadrant of the  $R_y - R_z$  plane with both  $R_y$  and  $R_z$  decreasing. Defining, as is standard

$$\tan \theta = \frac{R_z}{R_y}, \quad \tan \psi = \frac{dR_z}{dR_y} \quad (86)$$

we find that the trajectories satisfy

$$\frac{dR_z}{dR_y} = \frac{f(V_z, V_y)}{f(V_y, V_z)} \cot^2 \theta, \quad (87)$$

or in terms of volumes:

$$\frac{dV_z}{dV_y} = \frac{f(V_z, V_y)}{f(V_y, V_z)}. \quad (88)$$

It is immediately apparent that if  $f$  is symmetric, i.e.

$$f(V_z, V_y) = f(V_z, V_z) \quad (89)$$

then we have

$$\frac{dV_z}{dV_y} = 1, \quad (90)$$

that is the trajectories are straight lines in the  $V_y, V_z$  plane making an angle of  $\frac{\pi}{4}$  with the axes. By using  $V_y = \frac{4\pi}{3}R_y^3$  and  $V_z = \frac{4\pi}{3}R_z^3$ , these can be transferred to the  $[R_z, R_y]$  plane where straight lines become curves which in the downward direction move away from the straight line  $R_z = R_y$ . It follows that if the volume weight function  $f(V_y, V_z)$  is symmetrical then the self-dual trajectory defined by  $R_y = R_z$  is unstable within the class of spherical flows. Beyond showing that

asymmetry is a necessary condition for the stability for the self-dual flows, we also show a simple example where it is also sufficient. If we assume that

$$f(V_y, V_z) = \left(\frac{V_y}{V_z}\right)^p \quad (91)$$

then we have

$$\frac{dR_z}{dR_y} = \tan \psi = (\tan \theta)^{2(3p-1)}. \quad (92)$$

If  $p < \frac{1}{3}$  and the trajectory lies above the diagonal line  $\theta = \frac{\pi}{4}$ , then its slope  $\psi$  is less than  $\frac{\pi}{4}$  and it will move away from the diagonal. If the trajectory lies below the diagonal then its slope  $\psi$  is greater than  $\frac{\pi}{4}$  and it will again move away from the diagonal. Thus if  $p \leq \frac{1}{3}$  the self-dual flow is unstable and if  $p > \frac{1}{3}$  it will be stable.

As pointed out in [5], friction can stabilize attractors in the geometric self-dual flows in the  $[y_1, y_2]$  space of box ratios. Here we would like to point out that in case of volume-weighted spherical flows, friction also contributes to the relative stabilisation of size in the sense that the particle's linear size converges to each other. Since we treat friction as an individual abrasion, any monotonically increasing volume weight function  $f^f(V_y)$  associated with friction produces an asymmetry which has an analogous effect to the above-discussed asymmetry of the volume weight function for collisional abrasion.

In the next section we show that asymmetric models (although more complex than (91)) emerge naturally from physical considerations. We will only prove the stabilising property of the physical volume weight functions for the spherical case, however, they appear to have the same effect for general geometries.

## 6.4 Derivation of the volume weight function from physical models in the Bloore equations

We assume that volume evolution is given by an independent physical model as

$$\dot{V}_y^p = C_y^c g^c(V_y, V_z) \quad (93)$$

$$\dot{V}_z^p = C_z^c g^c(V_z, V_y). \quad (94)$$

where the superscript  $p$  stands for "physical" and the constants  $C_y^c, C_z^c$  may differ due to the different hardness of the material of the particles. In the spherical flows we can use (57) to obtain the volume weight function as

$$f(V_y, V_z) = \frac{C_y^c g^c(V_y, V_z)}{4a\pi(R_y + R_z)^2}. \quad (95)$$

Using (95), (75)-(76) can be written as

$$-\dot{R}_y = \frac{C_y^c g^c(V_y, V_z)}{4a\pi(R_y + R_z)^2} \left(1 + 2\frac{R_z}{R_y} + \left(\frac{R_z}{R_y}\right)^2\right) \quad (96)$$

$$-\dot{R}_z = \frac{C_z^c g^c(V_z, V_y)}{4a\pi(R_y + R_z)^2} \left(1 + 2\frac{R_y}{R_z} + \left(\frac{R_y}{R_z}\right)^2\right). \quad (97)$$

Later we give examples for some specific functions  $g^c(V_y, V_z)$ .

## 6.5 Derivation of the volume weight function from physical models in the box equations

Without giving any specific physical abrasion model, in this subsection we show how the volume weight functions  $f^c, f^f$  can be formally derived if such models are available. Later on, we give specific examples of some physical models, however, any physical model can be plugged into the equations of this subsection. We only assume that the physical model is defined by volume evolution equations for collisional and frictional abrasion, respectively, as

$$\dot{V}_y^{p,c} = C_y^c g^c(\mathbf{y}, \mathbf{z}) \quad \dot{V}_y^{p,f} = C_y^f g^f(\mathbf{y}) \quad (98)$$

$$\dot{V}_z^{p,c} = C_z^c g^c(\mathbf{z}, \mathbf{y}) \quad \dot{V}_z^{p,f} = C_z^f g^f(\mathbf{z}), \quad (99)$$

then by using (82)-(83) and (85) we can set the geometric and physical volume evolution rates to be equal and this condition yields:

$$f^c(\mathbf{y}, \mathbf{z}) = \frac{C_y^c g^c(\mathbf{y}, \mathbf{z})}{F^{g,c}(\mathbf{y}, \mathbf{z})} \quad (100)$$

$$f^f(\mathbf{y}) = \frac{C_y^f g^f(\mathbf{y})}{F^{g,f}(\mathbf{y})} \quad (101)$$

and  $F^{g,c}$  and  $F^{g,f}$  are given in (63) and (65), respectively. So, based on the above equations and (80)-(81) and (84), the box equations for the combined model (including the physical law for volume evolution) are

$$\dot{\mathbf{y}} = \frac{C_y^c g^c(\mathbf{y}, \mathbf{z})}{F^{g,c}(\mathbf{y}, \mathbf{z})} \mathbf{F}^c(\mathbf{y}, \mathbf{z}) + \frac{C_y^f g^f(\mathbf{y})}{F^{g,f}(\mathbf{y})} \mathbf{F}^f(\mathbf{y}, \nu_s, \nu_r) = \mathbf{F}^u(\mathbf{y}, \mathbf{z}) \quad (102)$$

$$\dot{\mathbf{z}} = \frac{C_z^c g^c(\mathbf{z}, \mathbf{y})}{F^{g,c}(\mathbf{z}, \mathbf{y})} \mathbf{F}^c(\mathbf{z}, \mathbf{y}) + \frac{C_z^f g^f(\mathbf{z})}{F^{g,f}(\mathbf{z})} \mathbf{F}^f(\mathbf{z}, \nu_s, \nu_r) = \mathbf{F}^u(\mathbf{z}, \mathbf{y}), \quad (103)$$

where  $\mathbf{F}^c, \mathbf{F}^f$  are defined in (34), (39) and (53), respectively and  $F^{g,c}, F^{g,f}$  are given in (63),(65).

## 7 Collective abrasion

Using the above model, a Markov-process can be simulated by regarding  $\mathbf{y}, \mathbf{z}$  in (102)-(103) as random vectors with *identical* distributions since they represent two random samples of the same pebble population. The evolution of this Markov process (and thus the time evolution of of the pebble size and ratio distributions) is of prime interest since it determines the physical relevance of the stable attractors identified in [5]. While the analytical investigation of the Markov process is beyond the scope of this paper, direct simulations are relatively straightforward. We consider  $N$  pebbles out of which we randomly draw two with coordinates  $\mathbf{y}^0, \mathbf{z}^0$  and run equations (102)-(103) for a short time period  $\Delta t$  on these initial conditions to obtain the updated vectors  $\mathbf{y}^1, \mathbf{z}^1$ . In the simplest linear approximation we have the recursive formula

$$\mathbf{y}^{i+1} = \mathbf{y}^i + \Delta t \mathbf{F}^u(\mathbf{y}^i, \mathbf{z}^i) \quad (104)$$

$$\mathbf{z}^{i+1} = \mathbf{z}^i + \Delta t \mathbf{F}^u(\mathbf{z}^i, \mathbf{y}^i). \quad (105)$$

Such an iterative step can be regarded as the cumulative, averaged effect of several collisions between the two selected pebbles. Apparently, the  $N = 2, \Delta t \rightarrow 0$  case is identical to (102)-(103). In [5] we investigated the behaviour of the deterministic flows in the special cases of steady state flows (31)-(32) and self-dual flows (42). Multi-body simulations allow the numerical study of the statistical stability of the flows, i.e. one can assess the stability of the above-mentioned special cases.

## 8 Physical models of mass evolution

It appears to be widely believed that the relationship between volume  $V$  and time  $t$  follows an exponential law suggested by Sternberg [4]

$$V(t) = V(0)e^{-\frac{t}{t_0}}, \quad (106)$$

where  $t_0$  is a constant. More accurately, Sternberg's Law is usually held to hold for the volume of pebbles as a function of distance along a river or stream. If they are transported along the river at constant speed this is equivalent to (106).

Our goal is to introduce physical collisional models which, on one hand, predict infinite lifetimes (in accordance with Sternberg), on the other hand, they can be plugged into the geometric equations via the formulae (102)-(103). We propose first collisional models followed by frictional models.

### 8.1 Collisional Models

It seems intuitively reasonable that that mutual abrasion will be greater the greater the kinetic energy  $E_{\text{com}}$  of the colliding particles in their common rest frame. This is given by

$$E_{\text{com}} = \frac{1}{2} \frac{m_y m_z}{m_y + m_z} u^2 \quad (107)$$

where  $u$  is the relative velocity of the abrader and the abraded and  $m_y$  and  $m_z$  are the masses of the pebbles. These will be related to the densities  $\rho_y$  and  $\rho_z$  and volumes by

$$m_y = \rho_y V_y, \quad m_z = \rho_z V_z. \quad (108)$$

For a homogeneous ensemble of pebbles it is reasonable to assume  $\rho_y = \rho_z$ . In binary collisions one might suppose that the rate of reduction of volume is proportional to  $E_{com}$  and a power  $\alpha$  of the mass. Assuming equal densities and that  $u^2$  is on average a constant, we arrive at the equation for *physical volume evolution*

$$-\dot{V}_y^{c,p} = C_y^c V_y^\alpha \frac{V_y V_z}{V_y + V_z} = C_y^c g^c(V_y, V_z) \quad (109)$$

$$-\dot{V}_z^{c,p} = C_z^c V_z^\alpha \frac{V_y V_z}{V_y + V_z} = C_z^c g^c(V_z, V_y) \quad (110)$$

where the superscript  $p$  stands for "physical" and the constants  $C_y^c, C_z^c$  may differ due to the different hardness of the material of the particles. This results in

$$\frac{dV_z}{dV_y} = \frac{C_z^c}{C_y^c} \left( \frac{V_z}{V_y} \right)^\alpha. \quad (111)$$

We remark that one plausible motivation behind (109)-(110) is Weibull Theory for fragmentation [35] [7] relating the material strength  $\sigma_{crit}$  to the specimen mass  $m$  as

$$\sigma_{crit} = \sigma_0 \left( \frac{m}{m_0} \right)^{-\frac{1}{\mu}} \quad (112)$$

where  $\sigma_0$  is the strength of the specimen of unit volume  $m_0$  and  $\mu$  is Weibull's modulus. This formula is based on the statistical distribution of Griffith cracks [6] and  $\mu \rightarrow \infty$  corresponds to homogeneous material without Griffith cracks. Here we assume that the critical fragmentation energy  $E_f$  per fragmented mass  $m_f$ , given as

$$\tau_{crit} = \frac{E_f}{m_f} \quad (113)$$

follows a similar power law

$$\tau_{crit} = \tau_0 \left( \frac{m}{m_0} \right)^{-\frac{1}{\bar{\mu}}} \quad (114)$$

and similarly to Weibull's modulus,  $\bar{\mu} \rightarrow \infty$  corresponds to homogeneous material. Using equations (107),(112) and (113) yields (109)-(110) with  $\alpha = 1/\bar{\mu}$ . Note that  $\alpha = 0$  corresponds to homogeneous material. As pointed out in [7], brittle materials are *softening* in fragmentation in the sense that the energy per unit fragmented volume is decreasing with the size of the particle. This behaviour implies in (109)-(110)

$$\alpha \geq 0. \quad (115)$$

In the box equations, via (58)-(59), (109)-(110) is translated into

$$-\dot{V}_y^{c,p} = C_y^c g^c(\mathbf{y}, \mathbf{z}) \quad (116)$$

$$-\dot{V}_z^{c,p} = C_z^c g^c(\mathbf{z}, \mathbf{y}) \quad (117)$$

which can be plugged into (102)-(103). In the spherical case we have

$$g^c(R_y, R_z) = \left( \frac{4\pi}{3} \right)^{1+\alpha} \frac{R_y^{3(1+\alpha)} R_z^3}{R_y^3 + R_z^3} \quad (118)$$

and using (119) this yields for the volume weight function

$$f(V_y, V_z) = \frac{C_y^c}{3a} \left( \frac{4\pi}{3} \right)^\alpha \frac{R_y^3 R_z^3}{(R_y^3 + R_z^3)} \frac{R_y^{3\alpha}}{(R_y + R_z)^2} \quad (119)$$

By substituting (118) into (96) we get the physical evolution equations for spheres.

We also note that (119) is asymmetrical:  $f(V_y, V_z) \neq f(V_z, V_y)$ . Indeed, in the case of spheres, (109)-(110) yield

$$\frac{dR_z}{dR_y} = \left( \frac{R_z}{R_y} \right)^{3\alpha-2} \quad (120)$$

and we can immediately see that the self-dual trajectory  $R_y = R_z$  will therefore be unstable unless  $\alpha > \frac{2}{3}$ . Recalling that the exponent  $\alpha$  was motivated by Weibull theory, this condition suggests that, in the absence of other effects, for nearly homogeneous particles the self-dual flows will be unstable.

## 8.2 Frictional models

Here we describe the evolution of mass as a single particle  $K_y$  is being abraded by friction and we postulate

$$-\dot{m}_y = \bar{C}_y^f m_y^\beta, \quad \bar{C}_y^f > 0 \quad (121)$$

which, for  $\beta = 1$  is essentially a simplified version of Archard's formula [18] by assuming constant velocity and contact area with the abrading surface. If the contact stress approaches the yield stress then higher  $\beta$  values may be appropriate. The case  $\beta \geq 1$  corresponds to infinite time horizon and, as we will show in the next subsection, the volume evolution equations (109)-(110) also predict similar behaviour, so for  $\beta \geq 1$  the two effects (collisional and frictional abrasion) may compete on the same timescale. In equation (121),  $\beta \geq 1$  can be motivated by assuming friction caused entirely by the gravity acting on the particle  $K_y$ , e.g. the particle is sliding on a free surface. Friction could also occur inside granular assemblies under compressive forces far exceeding the particles own weight; in this case mass will decay in finite time and frictional abrasion will dominate the whole process. However, as we showed in [5], only the continuous interaction of collisional and frictional abrasion can produce the geologically observed dominant pebble box ratios. Based on (121) we have

$$-\dot{V}_y^{p,f} = C_y^f V_y^\beta = C_y^f g^f(V_y) \quad (122)$$

where  $C_y^f = \bar{C}_y^f / \rho_y$  and again, the superscript  $p$  refers to the fact that this evolution is based on physical considerations rather than geometrical ones, superscript  $f$  refers to the frictional process. In the box equations (122) translates into

$$-\dot{V}_y^{p,f} = C_y^f V_y^\beta = C_y^f (8y_1 y_2 y_3^3)^\beta = C_y^f g^f(\mathbf{y}) \quad (123)$$

which can be plugged into (102).

## 8.3 Collective abrasion: rescaling of time

In section 7 we introduced the concept of collective abrasion. In case of two particles under mutual collisions we have assumed that in equal time intervals equal number of collisions occur. If we consider a collection of particles from which we choose random pairs and evolve them under the above-described binary process then the choice of this pairs can follow various rules, in any case, we have to consider that the probability of collision in equal time between two arbitrary particles is not equal. For example, it is a plausible assumption that in the same amount of time a large particle will suffer more collisions than a small particle. We will implement the particular assumption that the number  $N_y$  of collisions per unit time suffered by the particle  $\mathbf{y}$  is proportional to the  $\nu$ -power of the relative volumes:

$$N_y \propto \left( \frac{V_y}{V_z} \right)^\nu. \quad (124)$$

Needless to say, this assumption would not make sense in the binary process since from it would follow that the two colliding particles suffer different number of collisions in equal time intervals. Nevertheless, in case of collective abrasion this assumption can be implemented and in essence it requires the rescaling of time. If we denote the time in the collective process by  $T$  and time in the original, binary process by  $t$  then we have

$$\frac{dT}{dt} = \left( \frac{V_y}{V_z} \right)^\nu. \quad (125)$$

If we study the collective process (104)-(105) process then rescaled time can be implemented by modifying (109)-(110) as

$$-\dot{V}_y^{c,p} = C_y^c \frac{V_y^{(\alpha+\nu+1)} V_z^{(1-\nu)}}{V_y + V_z} = C_y^c \bar{g}^c(V_y, V_z) = C_y^c \bar{g}^c(\mathbf{y}, \mathbf{z}) \quad (126)$$

$$-\dot{V}_z^{c,p} = C_z^c \frac{V_z^{(\alpha+\nu+1)} V_y^{(1-\nu)}}{V_y + V_z} = C_z^c \bar{g}^c(V_z, V_y) = C_z^c \bar{g}^c(\mathbf{z}, \mathbf{y}). \quad (127)$$

As a consequence, if we model collective abrasion then in (102)-(103)  $g^c(\mathbf{y}, \mathbf{z})$  has to be replaced by  $\bar{g}^c(\mathbf{y}, \mathbf{z})$  and all other formulae remain unchanged.

## 9 Lifetimes, Sternberg's Law and the stability of the self-dual flows

### 9.1 Lifetimes, physical mass evolution models and Sternberg's Law

Bloore's geometric equation apparently predicts finite lifetimes for abrading particles, this is immediately suggested by the constant term on the right hand side of (1). However, not only the constant, but every single term in the geometric equation predicts finite time horizon for the particle and this property is inherited by the box equations, we discuss this in Appendix 12.

Our box model (102)-(103) is constructed in such a way that geometric volume evolution rates  $F^{g,c}, F^{g,f}$  (given in (63),(65)) are completely suppressed and volume evolution is determined by the physical evolution rates given in (98)-(99). Consequently, the lifetimes for the unified box model (102)-(103) are determined by the lifetimes for the physical volume evolution models (98)-(99) and next we study the latter. As we are about to show, they predict exponential decay for the volume, thus reproducing the empirical law (106) of Sternberg [4]. Needless to say, these models are certainly not unique and others may have similar properties.

We gave two examples of physical evolution models for collisional abrasion in (109)-(110) and (126)-(127). Since the former is just the  $\nu = 0$  special case of the latter it suffices to study the latter. We introduce a simple

**Lemma** *The differential equation  $\dot{f} = -cf^\gamma$  (with  $c = \text{constant} > 0, f(t_0) > 0, \gamma \neq 1$ ) has a solution  $f(t) = \left( f^{1-\gamma}(t_0) - (1-\gamma)(t-t_0) \right)^{1/(1-\gamma)}$  for  $t \geq t_0$ . Thus if  $\gamma < 1$ ,  $f(t)$  goes to zero in finite time, whereas if  $\gamma > 1$ , then  $f(t)$  reaches zero only after an infinite time.*

Similar conclusions could be reach if  $c(t)$  varies with time, with  $c(t-t_0)$  replaced by  $\int_{t_0}^t c(t)dt$ . In particular, if  $c(t) \rightarrow 0$  and  $\gamma > 1$  then we also have infinite time horizon. Equation (122) describes mass and volume evolution under friction, trivially agree with the equation in the Lemma and for  $\beta > 1$  it corresponds to processes with infinite lifetimes. Next we consider equations (126)-(127) for mass evolution under collisional abrasion. We note that in (126)-(127) both variables are strictly monotonically decreasing, regardless of the initial values. This implies that two cases are possible: (I) either  $V_y$  or  $V_z$  will approach zero while the other volume is still finite or (II) when both volumes approach zero simultaneously at some slope  $V_z/V_y = c_0$ .

**Case (I)** Assume  $V_y$  approaches zero first and thus we have  $V_y \ll V_z$ . Then, if  $\nu = 0$ , equation (126) for  $\dot{V}_y$  may be approximated by the equation in the lemma, by setting  $f = V_y, \gamma = \alpha + 1, c = -C_y^c$ . By assumption (115),  $\alpha \geq 0$  and so in all cases  $\gamma \geq 1$ . It follows that the lifetime for the  $\mathbf{y}$  particle is always infinite, approaching  $V_y = 0$  asymptotically. As  $V_y$  is asymptotic to zero, based on (127) so is  $\dot{V}_z$ , so the  $\mathbf{z}$  particle will also have infinite time horizon (approaching finite constant mass). If  $\nu \geq 0$  then we have  $c(t) = (V_y/V_z)^\nu$  and since  $V_y \rightarrow 0$  we also have  $c(t) \rightarrow 0$  so this also yields infinite time horizon for both particles.

**Case (II)** If  $V_y$  and  $V_z$  vanish together at some slope  $V_z/V_y = c_0$  then we can take either to equal  $f$  in the lemma and  $\gamma = \alpha + 1, c = -c_0 C_y^c / (c_0 + 1)$  or  $c = -c_0 C_z^c / (c_0 + 1)$ . The same conclusion holds.

### 9.2 Lifetimes and the volume weight functions

Field observations of river pebbles are consistent with Sternberg's Law [4] which predicts that particles live for ever. This gives an important constraint on evolution laws. In our model, the latter determine the volume weight functions and next we shall give some general results on whether or not a volume weight function predicts a finite lifetime by giving a general upper bound on the lifetime.

In the spherical case, based on (75) we can write

$$-\dot{R}_y \geq f(V_y, V_z) \quad (128)$$

and so we have

$$\frac{R_y(t)}{R_y(0)} \leq e^{-\int_0^t \frac{f(V_y, V_z)}{R_y} dt'} \quad (129)$$

which gives exponential decay as long as  $\frac{f(V_y, V_z)}{R_y}$  converges for small  $R_y$ . In the general case we may obtain volume evolution by integrating (128) over the surface  $\Sigma$ :

$$-\dot{V}_y \geq \int_{\Sigma} f(V_y, V_z) dA = A_y f(V_y, V_z). \quad (130)$$

Thus we have

$$\frac{V_y(t)}{V_y(0)} \leq e^{-\int_0^t f(V_y, V_z) \frac{A_y}{V_y} dt'} \quad (131)$$

which gives exponential decay as long as  $f(V_y, V_z) \frac{A_y}{V_y}$  converges for small  $V_y$ .

### 9.3 Stability of the self-dual flows in the stochastic process

We can study the evolution of  $\rho = V_y/V_z$  under the described process and we can see that  $\rho = 1$  is always a solution of (126)-(127). The stability of this solution is of particular interest since it indicates the stability of the self-dual flows in (102)-(103). It is easy to see that the stability of  $\rho = 1$  is guaranteed if

$$(1 - \rho)\dot{\rho} > 1 \quad (132)$$

and we can see from (126)-(127) that the condition for stability is

$$\alpha + 2\nu > 1. \quad (133)$$

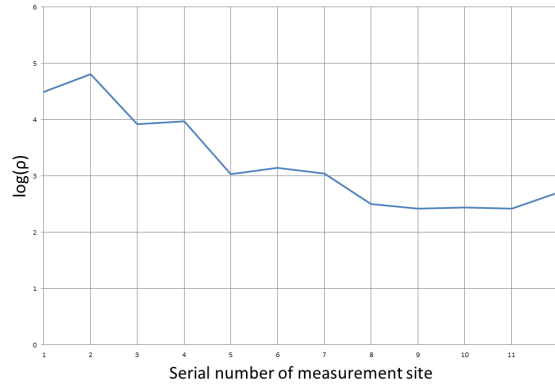


Figure 1: Field data from the Williams river

Now, we expect  $\alpha \ll 1$  if the material is nearly homogeneous; this suggests that the self-dual flows are not stable in the binary process where  $\nu = 0$ . In other words, our model predicts that the mass ratio of two, mutually abrading particles will diverge if the material is sufficiently homogeneous. On the other hand,  $\nu = 2/3$  is a plausible assumption, relating the number of collisions per unit time to the effective cross section of the particle. So, in a collective process we expect that the self-dual flows will be stable and attractive. This is also confirmed by the field data collected along the Williams river where we measured  $\bar{\rho} = V_{max}/V_{min}$  in each sample. Since  $\bar{\rho}$  is an upper bound for  $\rho$ , its evolution indicates the stability of the  $\rho = 1$  solution. In Figure 1 we plotted  $\log(\bar{\rho})$  versus the serial number of the measurement site along the Williams river, the latter can be regarded as an approximate measure of time. As we can see,  $\log(\bar{\rho})$  shows a marked decrease along the river thus indicating the stability of the  $\rho = 1$  solution.

These considerations also imply that our conclusions regarding the role of segregation in [5] are only valid for the geometric equations. If we study the unified flows then we expect that under the combined effect of collisions and friction, stable attractors in the space  $[y_1, y_2]$  of the box ratios will emerge spontaneously and robustly. Also, while segregation by size is catalysing this process, it is not a pre-condition for the emergence of the attractors. Rather, we expect that abrasion itself will further help to produce pebbles of similar sizes.

## 10 Acknowledgements

This research was supported by OTKA grant T104601. The comments from Dr Timea Szabó are greatly appreciated.

## References

- [1] F. J. Bloore, The Shape of Pebbles *Mathematical Geology* **9** (1977) 113-122
- [2] G. Domokos, A. Sipo and P. Várkonyi Formation of sharp edges and plane areas of asteroids by polyhedral abrasion *Astrophysical Journal* **699**(2009) L13-116
- [3] K. Brakke, *The motion of a surface by its mean curvature* Princeton University Press (1978)
- [4] H. Sternberg, Untersuchungen uber Langen-und Querprofil geschiebefuhrender Flusse, *Z. Bauwes.* **25** (1875) 486 506.
- [5] G. Domokos and G.W. Gibbons, The evolution of pebble shape in space and time *Proceedings of the Royal Society London* **468** (2146) 3059-3079. (2012).
- [6] A.A. Griffith, The phenomena of rupture and flow in solids. *Philos. T. Roy. Soc. A*, **221**, 163-198. (1921).
- [7] O- Tsoungui, D. Vallet, J-C. Charmet and S. Roux, Size effects in single grain fragmentation *Granular Matter* **2** 19-27. (1999).
- [8] P. L. Várkonyi and G. Domokos A general model for collision-based abrasion *IMA J. for Applied Math.* **76** 47-56 (2011).
- [9] A. R. Forsyth *Lectures on the Differential Geometry of Curves and Surfaces* Cambridge University Press (1920)
- [10] G. Domokos, G. W. Gibbons, A. A. Sipo's Circular, stationary profiles emerging in unidirectional abrasion [arXiv:1206.1589 Geophysics (physics.geo-ph)]
- [11] A. A. Sipo, G. Domokos, A. Wilson and N. Hovius A Discrete Random Model Describing Bedrock Erosion *Mathematical Geosciences* **43** (2011) 583-591, DOI: 10.1007/s11004-011-9343-8
- [12] G. Domokos, A. Sipo and P. Várkonyi Continuous and discrete models for abrasion processes *Periodica Polytechnica Architecture* **40** (2009) 3-8
- [13] B. van-Brunt and K. Grant, Potential applications of Weingarten surfaces in CAGD. *Computer Aided Geometric Design* **13** (1996) 569-582
- [14] W. .J. Firey, The shape of worn stones, *Mathematika* **21**(1974) 1-11
- [15] Lord Rayleigh, Pebbles, natural and artificial. Their shape under various conditions of abrasion *Proc R.Soc Lond A* **181** (1942) 107-118
- [16] Lord Rayleigh, Pebbles, natural and artificial. Their shape under various conditions of abrasion *Proc R.Soc Lond A* **182** (1944) 321-334
- [17] Lord Rayleigh, Pebbles of regular shape and their production in experiment *Nature* **154** (1944) 161-171
- [18] J. F. Archard and W. Hirst, The wear of metals under unlubricated conditions *Proc R.Soc Lond A* **236** (1956) 397-416
- [19] K. Tso, Deforming a hypersurface by its Gauss-Kronecker- curvature, *Comm. Pure Appl. Math* **38** (1985) 867-882
- [20] B. Andrews, Guass curvature flow:the fate of rolling stones *Invet. Math.* **138** (1999) 151-161

- [21] B. Andrews, Contraction of convex hypersurfaces in Euclidean space, *Cal Var* **2** (1994) 151-171
- [22] B. Chow, Deforming convex hypersurfaces by the n-th root of the Gaussian curvature, *J Diff Geom* **22** (1985) 117-138
- [23] G. Huisken, Flow by mean curvature of convex surfaces into spheres *J Diff Geom* **20**(1984) 27-266
- [24] F. Rhines, K. Craig, and R. Dehoff, Mechanism of steady-state grain growth in aluminium, *Metallurgy and Materials Transactions* (1974) 413-425
- [25] O. C. Schnürer, Surfaces expanding by the inverse Gauss curvature flow *Journal für die reine und angewandte Mathematik (Crelles Journal)* **600** 2006) 117-134 [arXiv:math/0412297]
- [26] G. Domokos, A. Sipos and P. Várkonyi Continuous and discrete models for abrasion processes *Periodica Polytechnica Architecture* **40** (2009) 3-8
- [27] R. Schneider and W. Weil, *Stochastic and Integral Geometry* Springer-Verlag (2008)
- [28] M. Kardar, G. Parisi and Y.C. Zhang *Phys Rev Lett* **56**(1986) 889-892
- [29] M. Marsilli, A. Maritan, F. Toigo and J.B. Banavar, Stochastic growth equations and reparameterization invariance *Rev Mod Phys* **68** (1996) 963-983
- [30] A. Maritan, F. Toigo, J. Koplik and J.R. Banavar, Dynamics of Growing Interfaces *Phys Rev Lett* **69** (1992) 3193-3195
- [31] M. T. Batchelora , R .V . Burneb , B .I . Henry, and S.D. Watt, Deterministic KPZ model for stromatolite laminae, *Physica A* **282** (2000) 123-136
- [32] G. Monge, *Application de l'analyse à la géométrie* Paris (1807) reprinted by ellipses (1994)
- [33] R. Goldman, Curvature formulas for implicit curves and surfaces *Computer Aided Geometric Design* **22** (2005) 632-658
- [34] Szabó, T. Fityus, S. and Domokos, G: Abrasion model of downstream changes in grain shape and size along the Williams River, Australia. *J. Geophysical Research/Earth Surface*, Submitted.
- [35] W. Weibull, A statistical theory of the strength of materials, *Roy. Swed. Inst. Eng. Res.* **151** (1939).

## 11 Appendix: Uni-directional Bloore Flows and Weingarten Surfaces

Bloore originally proposed [1] his equation to describe the evolution of the surface of a pebble under *isotropic* bombardment by abraders. In the case of bedrock evolution for example, the abraders are *unidirectional* and a modification of his equation is required. The simplest modification is the insertion of an inclination factor  $\cos \theta$ , where  $\theta$  is the angle between the direction of the abraders and the normal of the abraded surface[10]. This amounts to replacing  $v$  by  $\frac{v}{\cos \theta}$  in the previous equations. In a previous paper [10] we showed how circular profiles evolving with constant speed  $u$ , sometimes called *translators* emerge as stable final states of the cylindrically symmetric (or planar) form of the unidirectional Bloore equation. This agreed with existing theoretical and experimental work described in [11, 12].

In this section we shall extend our earlier result to the full three-dimensional case. We find that the possible final states are in general Weingarten surfaces, that is [9] surfaces for which there is a functional relation between the two principal curvatures  $\kappa_1$  and  $\kappa_2$ . In the special case (1) the possible final states belong to a special class of Weingarten surfaces (sometimes called *linear*)<sup>1</sup>, whose mean curvature  $H$ , and Gauss curvature  $K$  satisfy the linear relation

$$f(1 + 2bH + cK) = u, \tag{134}$$

where,  $f, b, c$  are constants characterising the abraders, and  $u$  is the constant final speed. A possible test of the theory would be to examine the distribution of mean and Gauss curvature on an abraded rock face as a function of time. If governed by the unidirectional Bloore equation this distribution, when plotted in the  $K - H$  plane should concentrate on the straight line (134)

---

<sup>1</sup>Beware: Linear Weingarten surfaces are sometimes defined differently: such that there is a linear relation between the principle curvatures. This is not equivalent. Another terminology for what we call Linear Weingarten surfaces is *Special Weingarten Surfaces* or *SW surfaces*. However this use is by no means universal

## 11.1 Weingarten surfaces as translators

We choose, for concreteness, to work with the Monge representation in which the original Bloore equation is (22), but our result does not depend on that choice. The cosine  $\cos \theta$  between the normal and the positive  $z$  direction is given by

$$\cos \theta = \frac{1}{\sqrt{1 + h_x^2 + h_y^2}}. \quad (135)$$

Replacing  $v$  by  $\frac{v}{\cos \theta}$  in (22) gives

$$\dot{h} = v(\kappa_1, \kappa_2) \quad (136)$$

If  $u$  is the constant speed, we have

$$h = ut + z(x, y), \quad (137)$$

and therefore

$$u = v(\kappa_1, \kappa_2), \quad (138)$$

which shows that the translator must be Weingarten surface. In the special case (1) we obtain (134).

A simple example of a travelling front or translator solution is a sphere

$$h(x, y, t) = ut + \sqrt{R^2 - x^2 - y^2}, \quad u = f\left(1 + \frac{b}{R} + \frac{c}{R^2}\right) \quad (139)$$

If  $c = 0$  we obtain *surfaces of constant mean curvature*

$$H = \frac{1}{2} \frac{u - f}{fb} \quad (140)$$

The case  $u - f = 0$  gives

$$R_1 + R_2 = -\frac{c}{b} \quad (141)$$

If  $b = 0$  then

$$fc \frac{1}{R_1 R_2} = u - f \quad (142)$$

which are surfaces of constant curvature. If  $\frac{1}{4}\Delta = f^2 b^2 - (f - u)fc$  then if  $\Delta > 0$  the linear Weingarten surface is called *elliptic*, if  $\Delta < 0$  it is called *hyperbolic* and if  $\Delta = 0$  it is called *tubular*. In particular, a surface of constant negative curvature is hyperbolic, while surfaces of constant positive curvature are elliptic, as are surfaces of constant mean curvature.

An example [13] of a hyperbolic surface of revolution given by

$$(x, y, z) = (\rho(u) \cos \phi, \rho(u) \sin \phi, z(u)) \quad (143)$$

with

$$\rho(u) = \sin u - \cos u, \quad z(u) = \cos u + \sin u + \ln\left(\frac{\sin u}{1 + \cos u}\right) \quad (144)$$

which satisfies

$$H + K + \frac{1}{2} = 0. \quad (145)$$

## 12 Appendix: Observable quantities in the geometric equations

We study particle shape evolution under collisional abrasion, governed by Bloore's partial differential equation (1) and we are concerned about qualitative and quantitative features of the evolution of the *observable quantities* such as linear size (maximal width), surface area and volume (denoted by  $D(t)$ ,  $A(t)$ ,  $V(t)$ , respectively) associated with convex solids in collisional abrasion governed by Bloore's partial differential equation (1). We refer to the three terms as the Eikonal, Mean Curvature and Gaussian term, respectively.

In (1), if coefficients  $b, c$  are constant then all observable quantities have finite lifetimes. If only one component of (1) is acting then we have:

$$\textbf{Eikonal: } \dot{D} = -1, \quad (146)$$

$$\textbf{Mean Curvature: } \dot{A} = -2b(W + 4\pi), \quad (147)$$

$$\textbf{Gaussian: } \dot{V} = -4\pi c. \quad (148)$$

where  $\dot{}$  refers to differentiation with respect to time  $t$  and  $W$  is the Wilmore functional given by

$$W = \int_{\Sigma} \frac{1}{4} \left( \frac{1}{R_1} - \frac{1}{R_2} \right)^2 dA \geq 0 \quad (149)$$

where  $R_i$  are the principal radii. In case of the box equations (39)-(40) we have the analogous observable quantities  $D_{box}, A_{box}, V_{box}$ , all given as functions of the dimensionless box ratios  $y_1, y_2$  multiplied by some power of  $y_3$ :

$$D_{box} = 2y_3 \quad (150)$$

$$A_{box} = 8y_3^2(y_1y_2 + y_1 + y_2) \quad (151)$$

$$V_{box} = 8y_3^3y_1y_2 \quad (152)$$

In case of the Eikonal, Mean Curvature and Gaussian flows we have

$$\text{Eikonal} : \dot{y}_3 = -2 \quad (153)$$

$$\text{Mean Curvature} : \dot{y}_3 = -\frac{1}{y_3} \left( \frac{y_1^2 + y_2^2}{2y_1y_2} \right) \quad (154)$$

$$\text{Gaussian} : \dot{y}_3 = -\frac{1}{y_3^2} \frac{1}{y_1^2y_2^2} \quad (155)$$

so, based on (150)-(155), the evolution speed for observable quantities is in all cases a product of an  $n$ -th power of  $y_3$  and some function  $f(y_1, y_2)$ :

$$\frac{d}{dt} \{Observable\} = y_3^n f(y_1, y_2) \quad (156)$$

The resulting values for  $n$  are summarised in Table 1 where we also list in  $\square$  brackets the power of length in the evolved observable quantity and the geometric quantity generating the evolution. The detailed formulae for  $f(y_1, y_2)$  we derive in section 12.2.

	$D_{box}$ [1]	$A_{box}$ [2]	$V_{box}$ [3]
<b>Eikonal</b> [0]	0	1	2
<b>Mean Curvature</b> [-1]	-1	0	1
<b>Gaussian</b> [-2]	-2	-1	0

Table 1: Value of  $n$  in equation (156) for 3 component flows in the box equations for 3 observable quantities. In  $\square$  brackets we indicated the power of the maximal size  $y_3$  in the given quantities.

## 12.1 Self-similar evolution

If we introduce the normalised observable quantities

$$\bar{D}(t) = D(t)/D(0), \quad \bar{A}(t) = A(t)/D(0), \quad \bar{V}(t) = V(t)/D(0), \quad (157)$$

then we assume that shapes remain self-similar then we have

$$\bar{A}(t) = \bar{D}^2(t), \quad \bar{V}(t) = \bar{D}^3(t) \quad (158)$$

and we have the similar relationship between normalised observable quantities in the box flows thus our previous results become comparable. We would like to stress that, except for the sphere, shapes do *not* evolve in a self-similar manner under these equations; we merely use this assumption to establish a qualitative correspondence between the results. We summarised the formulae in Table 2 and illustrated them in Figure 2

	$\bar{D}(t)$	$\bar{A}(t)$	$\bar{V}(t)$	timescale
<b>Eikonal</b>	$1 - t_e$	$(1 - t_e)^2$	$(1 - t_e)^3$	$t_e = C_e t$
<b>Mean Curvature</b>	$(1 - t_m)^{\frac{1}{2}}$	$1 - t_m$	$(1 - t_m)^{\frac{3}{2}}$	$t_m = C_m t$
<b>Gaussian</b>	$(1 - t_g)^{\frac{1}{3}}$	$(1 - t_g)^{\frac{2}{3}}$	$1 - t_g$	$t_g = C_g t$

Table 2: Evolution of normalised observable quantities under the assumption that shapes remain self-similar. Equations apply both in the Bloore PDE and the box flows, only the constants  $C_e, C_m, C_g$  differ. In the Bloore flows we have  $C_e = 2, C_m = 2b(W + 4\pi), C_g = 4\pi c$ . In case of unit spherical particles this yields  $C_e = 2, C_m = 16\pi \approx 50.16, C_g = 4\pi \approx 12.56$ . For the same problem in the box equations we get the constants  $C_{e,box} = 2, C_{m,box} = 48, C_{g,box} = 12$ , cf. equations (159),(163)and (167), respectively.

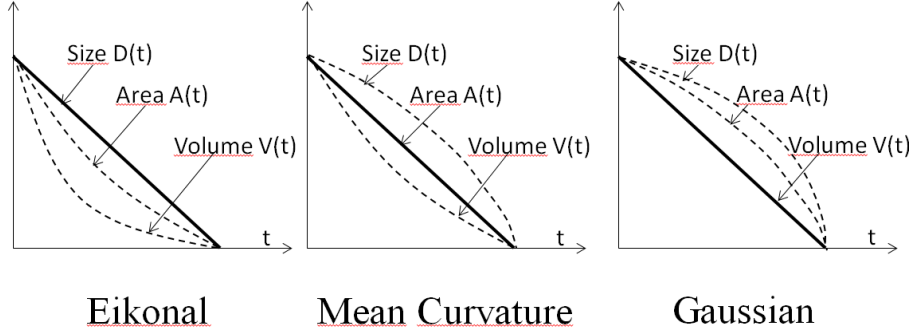


Figure 2: Qualitative evolution of observable quantities under the component flows. Each quantity is normalised by its initial value at  $t = 0$ . Solid line represent exact result for the PDE, dashed line represent qualitative curves under the assumption of self-similar evolution. We remark that the box equations yield the same results under these assumptions. We can observe *finite time horizon* in each case.

## 12.2 Observable quantities in the geometrical box flows

Here we investigate the evolution of observable quantities in the three component flows of (39)-(40).

### 12.2.1 Eikonal flow

If both curvature terms are zero then the box flows predict, similarly to the original PDE, linear size diminution, i.e. we have

$$\dot{D}_{box} = 2\dot{y}_3 = -2. \quad (159)$$

Unlike the original PDE, here we get explicit equations for the area and volume diminution as well:

$$\dot{A}_{box} = -16y_3(y_1 + y_2 + 1) \quad (160)$$

$$\dot{V}_{box} = -8y_3^2(y_1y_2 + y_1 + y_2) = -A_{box} \quad (161)$$

showing that both area and volume diminution is slowing down with time, however, from (159) it is clear that the particle has a finite time horizon. If we compare this to the PDE, we can observe that in case of volume evolution the continuous equations remain valid for polyhedra, however, this is not the case for area evolution. The naive explanation is that in case of volume evolution the role of the non-smooth parts (edges, vertices's) is negligible, the bulk of volume loss is occurring over the smooth (planar) faces and on those parts the smooth equation is valid. In case of surface area this argument is not true: under the Eikonal action, polyhedral surface is eliminated at the edges and therefore the non-smooth effects can not be neglected.

### 12.2.2 Mean Curvature Flow

If the Mean Curvature term dominates the flow then

$$\dot{D}_{box} = 2\dot{y}_3 = -\frac{2b}{y_3} \left( \frac{1}{y_1^2} + \frac{1}{y_2^2} \right) \quad (162)$$

$$\dot{A}_{box} = -4b \frac{2y_1^3 y_2^3 + y_1^3 y_2^2 + y_1^2 y_2^3 + y_1^3 y_2 + y_1 y_2^3 + y_1 y_2^2 + y_1^2 y_2 + 2y_1^3 + 2y_2^3}{y_1^2 y_2^2} \quad (163)$$

$$\dot{V}_{box} = -4b y_3 \left( \frac{y_1^2 + y_2^2 + y_1^2 y_2^2}{y_1 y_2} \right) \quad (164)$$

so, we see that by assuming constant box ratios  $y_1, y_2$  linear maximal size is diminishing at an accelerating rate. Similarly to the PDE, the evolution speed of the surface area is independent of maximal size, however, it is not a constant but it is approaching a negative constant as the box ratios approach 1. In case of the volume, again assuming constant box ratios, we see an accelerating decrease.

### 12.2.3 Gaussian Flow

If the Gaussian term dominates the flow then we have

$$\dot{D}_{box} = -\frac{c}{y_3^2} \left( \frac{1}{y_1^2 y_2^2} \right) \quad (165)$$

$$\dot{A}_{box} = -\frac{8c}{y_3} \left( \frac{y_1^4 y_2 + y_1 y_2^4 + y_1^4 + y_2^4 + y_1 + y_2}{y_1^2 y_2^2} \right) \quad (166)$$

$$\dot{V}_{box} = -8c \frac{y_1^3 + y_2^3 + 1}{y_1 y_2} \quad (167)$$

so we can see that, similar to the PDE, volume evolution is independent of size. Unlike in the PDE, here the speed is not constant, however, it is approaching a negative constant as the shape evolves towards the sphere.